SUPPLEMENT ARTICLE

Comparison of the Pathogenesis of the Angola and Ravn Strains of Marburg Virus in the Outbred Guinea Pig Model

Robert W. Cross,[1,2] Karla A. Fenton,[1,2] Joan B. Geisbert,[1,2] Hideki Ebihara,[3] Chad E. Mire,[1,2] and Thomas W. Geisbert[1,2]

[1]Department of Microbiology and Immunology, and [2]Galveston National Laboratory, University of Texas Medical Branch at Galveston; and [3]Rocky Mountain Laboratories, National Institute of Allergy and Infectious Diseases, National Institutes of Health, Hamilton, Montana

Background. Phylogenetic comparisons of known Marburg virus (MARV) strains reveal 2 distinct genetic lineages: Ravn and the Lake Victoria Marburg complex (eg, Musoke, Popp, and Angola strains). Nucleotide variances of >20% between Ravn and other MARV genomes suggest that differing virulence between lineages may accompany this genetic divergence. To date, there exists limited systematic experimental evidence of pathogenic differences between MARV strains.

Methods. Uniformly lethal outbred guinea pig models of MARV-Angola (MARV-Ang) and MARV-Ravn (MARV-Rav) were developed by serial adaptation. Changes in genomic sequence, weight, temperature, histopathologic findings, immunohistochemical findings, hematologic profiles, circulating biochemical enzyme levels, coagulation parameters, viremia levels, cytokine levels, eicanosoid levels, and nitric oxide production were compared between strains.

Results. MARV-Rav infection resulted in delayed increases in circulating inflammatory and prothrombotic elements, notably lower viremia levels, less severe histologic alterations, and a delay in mean time to death, compared with MARV-Ang infection. Both strains produced more marked coagulation abnormalities than previously seen in MARV-infected mice or inbred guinea pigs.

Conclusions. Although both strains exhibit great similarity to pathogenic markers of human and nonhuman primate MARV infection, these data highlight several key differences in pathogenicity that may serve to guide the choice of strain and model used for development of vaccines or therapeutics for Marburg hemorrhagic fever.

Keywords. filovirus; Marburg virus; Angola; Ravn; guinea pig; animal model; pathogenesis; coagulation.

Since the discovery of Marburg virus (MARV) during the original outbreak in 1967, it has caused sporadic outbreaks of severe hemorrhagic fever in Central Africa, with case-fatality rates (CFRs) ranging from 23% to 90% [1–3]. Research has focused on a handful of strains obtained from these outbreaks, with an emphasis on the Musoke, Ravn (MARV-Rav), and Angola (MARV-Ang) strains. The Musoke strain was first isolated in 1980 from a physician who survived nosoco- mial transmission from a patient infected in Nzoia, Kenya [4]. MARV-Rav was first isolated in 1987 from a case originating in southeastern Kenya but has been associated with large outbreaks of Marburg hemorrhagic fever (MHF) in the Democratic Republic of the Congo during 1998–2000, where strain-specific CFR metrics were impossible to enumerate because of concurrent circulation of multiple strains [1, 3]. MARV-Ang was responsible for the largest documented outbreak (252 cases) of MHF, in which a 90% CFR was reported, a rate very similar to that of the most virulent strains of Ebola virus [2].

Phylogenetic comparisons across MARV strains reveal 2 distinct genetic lineages: Ravn and the Lake Victoria Marburg complex (eg, Musoke, Ci67, Popp, and Angola strains), wherein nucleotide variances of >20%

Presented in part: 6th International Symposium on Filoviruses, Galveston, Texas, 30 March–2 April 2014.

Correspondence: Thomas W. Geisbert, PhD, University of Texas Medical Branch, Galveston National Laboratory, 301 University Blvd, Galveston, TX 77550-0610 (twgeisbe@utmb.edu).

The Journal of Infectious Diseases® 2015;212:S258–70

DOI: 10.1093/infdis/jiv182

between Ravn and other MARV genomes exist [2]. The level of genetic divergence and variation in CFR between strains suggest that these changes may contribute to variation in virulence. Many studies to characterize the pathogenesis of MARV infection have occurred since the original outbreak; however, some variability exists between these reports, depending on which strain of MARV was used [5–8]. This presents challenges for medical countermeasure development, such that inherent genetic differences may contribute to altered disease outcome across MARV strains, and thus any countermeasure or diagnostic assay may need evaluation across MARV strains.

Until recently, most MARV-specific countermeasures were tested in vivo, using mice or inbred strain 13 guinea pigs (GPs) [9–11]. Limitations in interpretation are necessary because delayed immunoresponsiveness and incomplete recapitulation of hallmark features of MHF (fever, diarrhea, weight loss, coagulopathies, vascular leak, and marked immune derangement similar to sepsis) may factor into the limited predictive value that these models have had to date [12]. Recently, we developed uniformly lethal outbred GP models for several strains of MARV by serial adaptation. These GP-adapted (GPA) MARV strains have demonstrated predictive efficacy in postexposure treatment in nonhuman primates (NHPs) [5, 13]. Here, we performed a temporal comparison of the events leading to death in outbred GPs infected with GPA MARV-Ang and MARV-Rav. We report not only remarkable similarities between MHF in NHPs and MHF in humans but also MARV strain-specific differences in virulence.

MATERIALS AND METHODS

Virus Adaptation

MARV-Ang and MARV-Rav strains were adapted to uniform lethality in outbred Hartley strain GPs by serial passage of virus isolated from infected livers and/or spleens and sequenced as outlined in the Supplementary Methods [14].

Inoculation of GPs

Animal studies were conducted under biosafety level 4 (BSL4) containment at the Galveston National Laboratory and were approved by the University of Texas Medical Branch (UTMB) Institutional Laboratory Animal Care and Use Committee. Female outbred Hartley strain GPs (weight, approximately 351–400 g) from Charles River Laboratories were quarantined upon receipt and acclimatized for approximately 1 week prior to MARV challenge. Forty animals were divided into 11 groups of 4 animals per group, with 5 groups per virus strain and 1 uninfected control group. Individual animals were challenged with approximately 5000 plaque-forming units (PFU) of GPA MARV-Ang or GPA MARV-Rav or mock challenged with Hanks' balanced salt solution with 2% fetal bovine serum, by intraperitoneal injection.

Necropsy

Each group of MARV-infected GPs was euthanized on postinfection days 1, 3, 5, or 7 or at a terminal point, when euthanasia criteria was met (n = 4/group/day). Clinical signs, weights, and transponder-mediated temperatures were recorded daily up to the time of euthanasia. Prior to necropsy, whole-blood, plasma (in ethylenediaminetetraacetic acid–lined tubes), and citrated plasma specimens were collected by cardiac puncture for hematologic analysis, serum/plasma biochemical assays, and viremia determination. Gross findings were documented, and select tissue specimens were aseptically removed and frozen at −70°C until analysis. The following tissue specimens were collected from all animals for histologic and immunohistochemistry analyses: liver, spleen, kidney, adrenal gland, lung, brain, lymph nodes (axillary, inguinal, mesenteric, and mandibular), salivary gland, trachea, esophagus, stomach, duodenum, ileocecal junction, colon, urinary bladder, reproductive tract, pancreas, haired skin, and heart.

Histologic and Immunohistochemistry Analyses

Selected tissues were fixed in formalin for at least 21 days in a BSL-4 facility. Specimens were then removed from the BSL-4 facility and processed in a BSL-2 facility, using routine histopathologic procedures, as outlined in the Supplementary Materials.

Hematologic Analysis, Serum Biochemistry Analysis, and Determination of Coagulation Parameters

Complete blood counts, analysis of coagulation dynamics, and analysis of blood chemistry parameters were performed on blood, serum, or plasma specimens. Analysis of select cytokines, coagulation factors, eicanosoids, and nitric oxide in serum or plasma specimens was also performed as detailed in the Supplementary Materials.

Virus Isolation

Determination of infectious virus in plasma, spleen, liver, kidney, adrenal, pancreas, lung, and brain tissue homogenates was made using standard plaque assays, as outlined in the Supplementary Materials.

Statistics Statement

Conducting animal studies in a BSL-4 facility severely restricts the number of animal subjects, the volume of biological samples that can be obtained, and the ability to repeat assays independently, thus limiting the power of statistical analysis. Consequently, data are presented as the mean values calculated from replicate samples, not replicate assays, and error bars represent standard deviations across replicates.

RESULTS

Adapted Virus Sequence Analysis

Sequence comparison of GPA MARV-Ang with the prototype strain (accession number DQ447653.1) revealed nucleotide substitutions resulting in a single amino acid change in VP40 and 2 changes in VP24, both viral matrix proteins. Three nucleotide changes were discovered in noncoding regions, and 2 silent mutations were detected in the polymerase gene. Comparison of GPA MARV-Rav with prototype MARV-Rav (accession number DQ447649.1) revealed nucleotide substitutions resulting in a single amino acid change in both NP and glycoprotein and 4 changes in VP40. One silent mutation in the polymerase gene was also detected. The resulting mutations may have been acquired during the consecutive passages in GPs and/or passages in Vero 76 cells during seed stock production (Table 1).

Virus Titers in Blood and Tissues

Plasma viremia was first detected on day 3 for both MARV-Ang and MARV-Rav strains, with equivalent titers of approximately 2.7 $\log_{10}$ PFU/mL. The peak MARV-Ang viremia level of approximately 7. 9 $\log_{10}$ PFU/mL on day 7 was maintained through terminal collections. The MARV-Rav viremia level peaked at approximately 6.4 $\log_{10}$ PFU/mL at terminal collection. Virus was recovered from spleen, pancreas, lung, kidney, liver, adrenal gland, and plasma from both MARV-Ang and MARV-Rav groups beginning on day 3, with higher titers detected in spleen, lung, and liver homogenates from the MARV-Ang group. On day 7, higher mean titers were recorded in liver and plasma from Marv-Ang–infected animals, whereas higher mean titers were observed in spleen, lung, kidney, and adrenal glands from MARV-Rav–infected animals. The highest titers in lung, kidney, adrenal gland, and plasma were measured at terminal collection in MARV-Ang–infected animals (Table 2).

Table 1. Genetic Changes in Guinea Pig–Adapted (GPA) Marburg Virus (MARV) Strains

Strain, Nucleotide	Base Change	Result	Gene
MARV-Angola			
2931	U>A	. . .	Noncoding
4735	U>A	N56K	VP40
10 402	G>A	V66I	VP24
10 853	U>C	L216S	VP24
13 115	U>C	Silent	L
17 249	U>A	Silent	L
18 713	C>A	. . .	Noncoding
19 105	A>U	. . .	Noncoding
MARV-Ravn			
143	A>U	T14S	NP
4647	U>C	L27S	VP40
4665	U>C	L33P	VP40
4725	U>C	F53S	VP40
4726	U>C	F53S	VP40
7118	G>C	G435A	Glycoprotein
13 787	U>C	Silent	L

The genome of GPA MARV-Ravn was compared with that of variant DQ447649.1, and the genome of MARV-Angola was compared with that of variant DQ447653.

Gross Findings

GPs from terminal groups were followed for mean changes in weights, temperature, and time to death. MARV-Ang–infected animals from this group met euthanasia criteria a mean of 1 day earlier than subjects from the MARV-Rav group (Figure 1*A*). Mean body weights at the time of necropsy were compared with initial weights, with comparable progressive weight loss between virus strain cohorts noted. Mean percentages changes in weights for MARV-Rav–infected GPs were −1.8% on day 5, −8.4% on day 7, and −25% at the terminal time point. MARV-Ang–infected animals began losing weight on day 6 (mean percentage change, −1.3%), with mean percentages changes of −6% on day 7 and −12.5% at terminal time points. MARV-Rav–infected animals had higher mean temperatures beginning on day 3 and remained at +1°C until day 7, when a peak of +1.5°C was followed by progressive hypothermia until time of death. MARV-Ang–infected animals had slowly progressive fevers that peaked at +1°C on day 6 and were also followed by hypothermia. Mock-infected control animals maintained stable weight and core temperature during the study (Figure 1*B*).

No gross lesions were present in the mock-infected control GPs (Figure 1*C*). Gross lesions present at necropsy of both MARV-Rav–infected GPs and MARV-Ang–infected GPs appeared on day 3 and increased in severity over the course of the study. The most significant gross lesions included splenic mottling with enlargement, multifocal to diffuse hepatic pallor, lymphadenomegaly, and gastrointestinal congestion with ulceration (Figure 1*D*–*F*). The severity of gastrointestinal and hepatic lesions in the terminal MARV-Ang–infected GPs (Figure 1*D* and 1*F*) were more prominent than those in the terminal MARV-Rav–infected GPs (Figure 1*E*). Detailed gross findings are available in the Supplementary Materials.

Hematologic Findings

Total and differential white blood cell counts for both strains of MARV elicited marked evidence of neutrophilia-mediated leukocytosis. Strikingly elevated circulating levels of neutrophils were noted beginning on 3 day and peaked on day 5 after infection for both strains. A concurrent marked lymphopenia was observed, as evidenced by declining mean lymphocyte counts. Thrombocytopenia, compared with control values, was marked, beginning at day 5 and continuing through terminal collection. Increases in mean platelet volume were also noted, beginning on day 5 and continuing through death for both infected

Table 2. Tissue and Plasma Marburg Virus (MARV) Burdens Over Time, by MARV Strain

	MARV Load, Log_{10} PFU/mL, Mean ± SD				
Tissue, Strain	Day 1	Day 3	Day 5	Day 7	Terminal Time Point
Brain					
Ravn	ND	ND	3.62 ± 0.46	4.71 ± 0.49	5.74 ± 0.49
Angola	ND	ND	3.37 ± 0.38	5.89 ± 0.42	5.01 ± 0.42
Spleen					
Ravn	ND	4.68 ± 0.44	6.35 ± 0.94	7.90 ± 0.60	7.19 ± 0.39
Angola	ND	5.27 ± 0.27	6.75 ± 0.38	6.95 ± 0.47	7.77 ± 0.51
Pancreas					
Ravn	ND	3.18 ± 0.62	5.03 ± 0.07	6.52 ± 0.64	6.14 ± 0.31
Angola	ND	2.65 ± 0.42	5.19 ± 0.49	6.34 ± 0.63	6.40 ± 0.36
Lung					
Ravn	ND	3.03 ± 0.33	5.32 ± 0.51	7.06 ± 0.46	6.08 ± 0.36
Angola	ND	4.00 ± 0.46	4.82 ± 0.28	6.25 ± 0.36	6.90 ± 0.43
Kidney					
Ravn	ND	2.75 ± 0.62	4.87 ± 0.51	6.80 ± 0.59	5.53 ± 0.41
Angola	ND	3.29 ± 0.37	4.72 ± 0.16	5.92 ± 0.51	7.71 ± 0.60
Liver					
Ravn	ND	4.21 ± 0.57	6.81 ± 0.36	7.84 ± 0.41	7.89 ± 0.50
Angola	ND	5.69 ± 0.45	5.79 ± 0.29	8.48 ± 1.08	8.01 ± 0.34
Adrenal					
Ravn	ND	3.30 ± 0.62	6.59 ± 0.61	7.88 ± 0.69	6.78 ± 0.63
Angola	ND	3.49 ± 0.39	5.51 ± 0.36	6.98 ± 0.50	7.64 ± 0.54
Plasma					
Ravn	ND	2.60 ± 0.48	5.96 ± 1.23	6.17 ± 0.43	6.36 ± 1.15
Angola	ND	2.88 ± 0.44	5.77 ± 0.52	7.97 ± 0.42	7.60 ± 0.40

Abbreviations: ND, not detected; PFU, plaque-forming units.

groups. Basophilia and eosinophilia began on day 5 and progressed through death (Table 3).

Serum Biochemistry Findings

No remarkable changes were noted in early serum enzyme levels but most were elevated in late disease. Beginning day 7 and continuing to death, remarkable 10-fold increases in circulating levels of aspartate transaminase and alkaline phosphatase were present in both MARV strains. More-modest increases in levels of alanine transaminase (approximately 2.5-fold) and gamma-glutamyl transpeptidase (approximately 6-fold) were detected at late-stage disease. The total bilirubin level was within normal limits until day 7, after which it doubled in MARV-Rav–infected animals and tripled in MARV-Ang–infected animals at termination time points. Blood urea nitrogen levels remained consistent throughout infection in MARV-Ang–infected animals; however, a 2-fold increase was observed at final time points in MARV-Rav–infected animals. Hypoalbuminemia with concurrent hypoproteinemia began on day 5 (Table 3).

Histopathologic and Immunohistochemistry Findings

Histopathologic lesions and immunoreactivity for MARV antigen in tissues of MARV-infected GPs were most apparent by day 3, with the severity of the lesions increasing over the duration of the study. MARV antigen associated with histologic lesion severity was similar between both MARV-Rav–infected animals and MARV-Ang–infected animals; however, infection by cell type was different, with obvious progression of up to 2 days sooner in the MARV-Ang group, compared with the MARV-Rav group. No significant histopathologic lesions, presence of viral antigen, or abnormal fibrin was observed in mock-infected control GP tissues.

Liver

Beginning on day 3, MARV antigen–positive Kupffer cells were observed for both MARV-Rav–infected GPs (3 of 4; Figure 2*B*) and MARV-Ang–infected GPs (4 of 4; Figure 2*D*). Additionally, minimal individualized hepatocytes (MARV-Rav–infected GPs) and small clusters of adjacent hepatocytes (MARV-Ang–infected GPs) had immunoreactivity. Lesions on hematoxylin and eosin (H/E)–stained sections associated with MARV antigen were detected on day 3, with hepatocellular degeneration/necrosis and sinusoidal leukocytosis in 3 of 4 MARV-Rav–infected GPs and 4 of 4 MARV-Ang–infected GPs. The prevalence of MARV antigen–positive Kupffer cells and clusters of hepatocytes increased throughout the study for

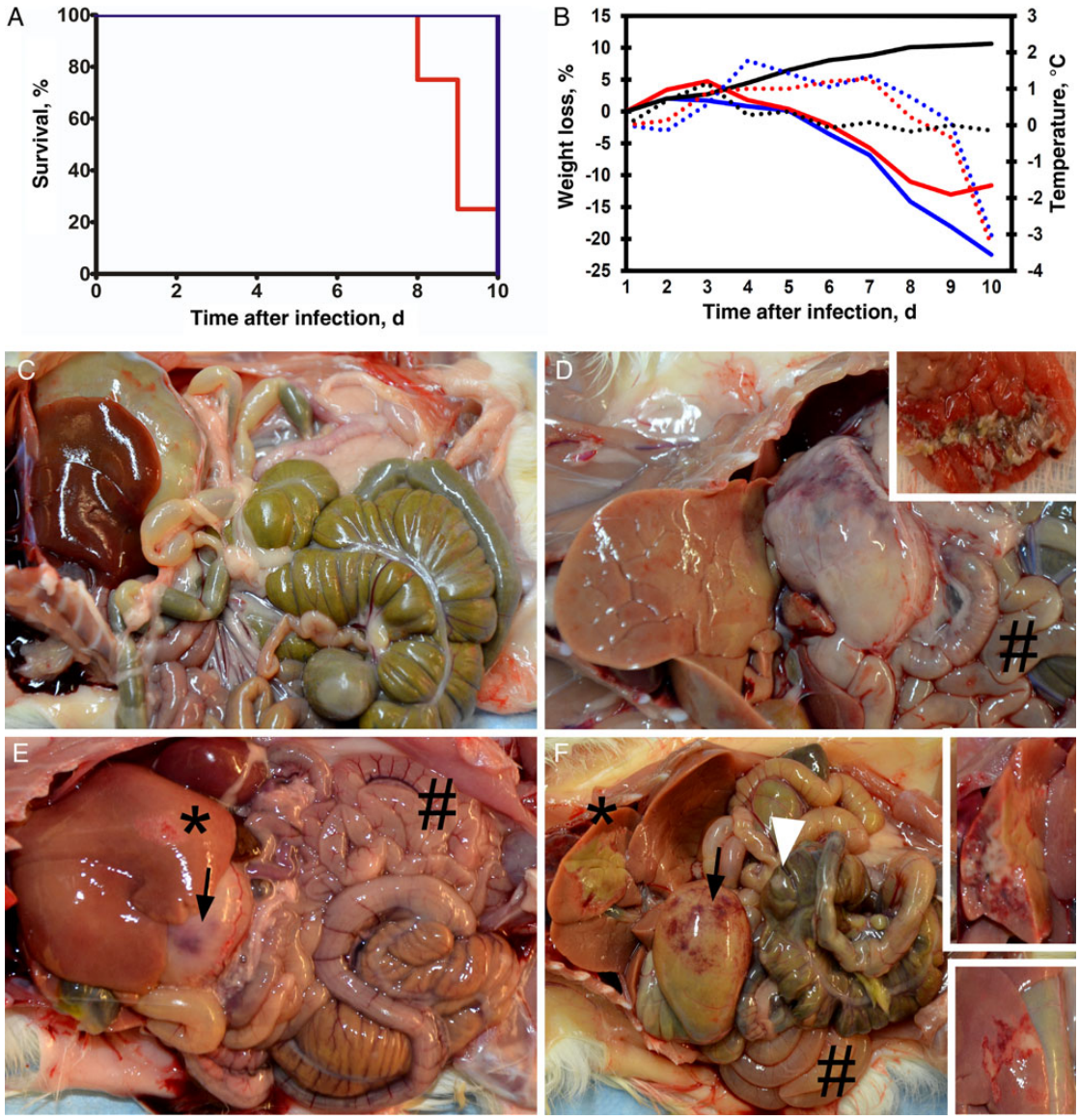

Figure 1. *A*, Survival curve of guinea pigs (GPs) infected with Marburg virus Ravn (MARV-Rav; blue line) and MARV-Angola (MARV-Ang; red line). *B*, Percentage weight loss and temperature during the study. MARV-Rav–infected GPs are represented by blue solid lines (weight) and dotted lines (temperature), Marv-Ang–infected GPs are represented by red solid lines (weight) and dotted lines (temperature), and control GPs are represented by black solid lines (weight) and dotted lines (temperature) lines. *C–F*, Comparison of the gross pathology of mock-infected control GPs (*C*), MARV-Rav–infected GPs (*E*), and MARV-Ang–infected GPs (*D* and *F*) at terminal time points. Gross lesions were noted in the MARV-Rav GPs (*E*) and MARV-Ang GPs (*D* and *F*), liver (black asterisk) moderate multifocal to diffuse pallor (hepatocellular degeneration/necrosis) (*E*), severe multifocal to diffuse pallor (hepatocellular degeneration/necrosis) (F insets), gastric congestion (black arrow), gastric ulceration (*D* inset), prominent lymphoid tissues (white arrowhead) (*F*), flaccid/fluid filled intestines (#) (*D*, *F* and *E*).

both MARV-Rav–infected GPs (12 of 12) and MARV-Ang–infected GPs (12 of 12). Progressive hepatocellular vacuolation, degeneration/necrosis with mineralization, and sinusoidal leukocytosis on H/E-stained sections corresponded with MARV antigen in all GP livers on day 5, day 7, and in terminal groups (12 of 12 in the MARV-Rav group and 12 of 12 in the MARV-Ang group). Councilman-like bodies were occasionally observed on day 5 in 2 of 4 MARV-Rav–infected GPs and 4 of 4 MARV-Ang–infected GPs and on day 7 in 1 of 4 MARV-Rav–infected GPs and 2 of 4 MARV-Ang–infected GPs (Figure 2*H* and 2*E*). Beginning on day 1 and progressing through death, MARV-Rav–infected animals displayed an earlier onset of marked increases in nuclear and cytoplasmic expression of high-mobility group B1 (HMGB-1) in Kupffer cells and hepatocytes as compared to MARV-Ang–infected GPs and control animals (Supplementary Figure 1*A–G*).

Table 3. Results of Hematologic and Serum Biochemistry Analyses

Parameter, Strain	Mean Value ± SD					
	Control	Day 1	Day 3	Day 5	Day 7	Terminal Time Point
Hematologic						
WBC count, ×1000 cells/μL	3.4 ± 1.6	. . .	. . .	. . .	. . .	. . .
Ravn	. . .	3.1 ± 1.2	2.6 ± 0.5	1.4 ± 0.5	3.2 ± 2.2	9.1 ± 1.6
Angola	. . .	3.3 ± 1.2	2.8 ± 0.4	3.7 ± 1.9	5.2 ± 2.6	7.1 ± 4.4
Neutrophils, %	36.8 ± 7.2	. . .	. . .	. . .	. . .	. . .
Ravn	. . .	41.7 ± 3.9	60.3 ± 7.7	61.2 ± 6.9	53.9 ± 8.1	57.3 ± 7.6
Angola	. . .	47.3 ± 10.7	60.7 ± 7.0	68.2 ± 10.2	50.9 ± 4.5	52.7 ± 4.0
Lymphocytes, %	59.3 ± 9.5	. . .	. . .	. . .	. . .	. . .
Ravn	. . .	55.8 ± 3.5	36.4 ± 8.1	31.8 ± 7.3	28.3 ± 4.0	29.8 ± 9.3
Angola	. . .	46.3 ± 12.2	37.0 ± 6.0	26.7 ± 11.9	33.6 ± 2.8	34.1 ± 5.4
Monocytes, %	2.0 ± 0.9	. . .	. . .	. . .	. . .	. . .
Ravn	. . .	1.2 ± 0.5	1.3 ± 1.2	3.1 ± 2.0	1.6 ± 1.2	0.5 ± 0.3
Angola	. . .	3.6 ± 2.5	2.0 ± 1.1	2.2 ± 0.5	1.5 ± 1.0	1.3 ± 0.7
Eosinophils, %	1.8 ± 1.6	. . .	. . .	. . .	. . .	. . .
Ravn	. . .	1.3 ± 1.4	2.0 ± 2.2	3.3 ± 1.4	12.8 ± 4.9	9.1 ± 1.8
Angola	. . .	2.9 ± 2.6	0.2 ± 0.1	2.6 ± 2.8	11.3 ± 1.4	8.9 ± 2.8
Basophils, %	0	. . .	. . .	. . .	. . .	. . .
Ravn	. . .	0	0	0.6 ± 0.4	3.4 ± 1.8	3.4 ± 0.7
Angola	. . .	0	0	0.4 ± 0.4	2.8 ± 0.6	3.0 ± 1.3
Platelet count, ×1000 platelets/dL	468.3 ± 23.7	. . .	. . .	. . .	. . .	. . .
Ravn	. . .	445.8 ± 69.0	390.0 ± 116.6	222.5 ± 65.5	187.8 ± 18.2	307.0 ± 83.5
Angola	. . .	446.3 ± 74.6	469.3 ± 102.4	228.3 ± 93.9	153.8 ± 62.5	228.5 ± 83.6
Mean platelet volume, fL	5.4 ± 0.6	. . .	. . .	. . .	. . .	. . .
Ravn	. . .	5.7 ± 0.4	6.0 ± 0.4	10.6 ± 0.8	10.2 ± 6.9	13.1 ± 0.6
Angola	. . .	5.8 ± 0.5	6.0 ± 0.4	9.9 ± 1.8	10.9 ± 2.2	13.2 ± 1.2
Clinical						
Albumin level, g/dL	4.3 ± 0.2	. . .	. . .	. . .	. . .	. . .
Ravn	. . .	4.3 ± 0.4	4.1 ± 0.3	3.6 ± 0.1	3.0 ± 0.3	0.4 ± 0.5
Angola	. . .	4.5 ± 0.1	4.3 ± 0.2	3.5 ± 0.3	1.2 ± 1.1	0.5 ± 0.1
Total protein level, g/dL	4.8 ± 0.1	. . .	. . .	. . .	. . .	. . .
Ravn	. . .	5.0 ± 0.6	5.0 ± 0.2	5.1 ± 0.2	4.8 ± 0.4	1.6 ± 0.7
Angola	. . .	5.0 ± 0.3	4.9 ± 0.2	4.8 ± 0.3	2.7 ± 1.2	1.9 ± 0.1
ALP level, U/L	190.5 ± 28.3	. . .	. . .	. . .	. . .	. . .
Ravn	. . .	183.5 ± 31.1	155.8 ± 24.2	489.8 ± 126.9	1613.0 ± 937.5	1393.8 ± 688.4
Angola	. . .	201.3 ± 16.9	187.3 ± 30.2	197.5 ± 59.7	1225.3 ± 381.5	1131.0 ± 208.7
ALT level, U/L	28.0 ± 5.9	. . .	. . .	. . .	. . .	. . .
Ravn	. . .	46.0 ± 10.1	31.3 ± 2.2	40.0 ± 8.0	80.0 ± 24.8	63.5 ± 34.9
Angola	. . .	45.0 ± 13.7	40.3 ± 14.5	42.5 ± 12.0	55.5 ± 21.3	60.5 ± 21.7
AST level, U/L	84.8 ± 34.4	. . .	. . .	. . .	. . .	. . .
Ravn	. . .	100.0 ± 54.3	63.8 ± 14.0	239.3 ± 51.8	1228.0 ± 610.5	1030.3 ± 506.1
Angola	. . .	115.3 ± 25.5	81.5 ± 17.8	201.8 ± 138.3	853.5 ± 285.7	692.0 ± 275.4
GGT level, U/L	7.0 ± 0.8	. . .	. . .	. . .	. . .	. . .
Ravn	. . .	7.3 ± 1.3	7.0 ± 0.8	14.5 ± 3.7	44.3 ± 22.3	35.8 ± 19.2
Angola	. . .	7.0 ± 0.8	6.8 ± 1.0	11.3 ± 4.2	39.3 ± 14.7	24.3 ± 15.1
Glucose level, mg/dL	187.3 ± 57.5	. . .	. . .	. . .	. . .	. . .
Ravn	. . .	225.5 ± 41.8	216.3 ± 39.5	184.3 ± 3.5	226.5 ± 45.4	51.5 ± 29.9
Angola	. . .	197.3 ± 45.8	211.8 ± 39.4	202.8 ± 36.8	118.0 ± 50.2	90.0 ± 19.6
Amylase level, U/L	1190.3 ± 129.0	. . .	. . .	. . .	. . .	. . .
Ravn	. . .	1550.0 ± 161.8	1000.0 ± 148.2	1016.0 ± 155.4	1342.3 ± 322.1	683.3 ± 304.0
Angola	. . .	1379.8 ± 274.2	1075.8 ± 259.3	956.0 ± 195.3	901.0 ± 282.0	719.3 ± 117.4

Table 3 continued.

Parameter, Strain	Mean Value ± SD					
	Control	Day 1	Day 3	Day 5	Day 7	Terminal Time Point
TBIL level, mg/dL	0.3 ± 0.1	. . .	. . .	. . .	. . .	. . .
Ravn	. . .	0.3 ± 0.0	0.3 ± 0.1	0.3 ± 0.1	0.6 ± 0.3	0.5 ± 0.2
Angola	. . .	0.3 ± 0.1	0.3 ± 0.0	0.3 ± 0.1	1.0 ± 0.6	1.3 ± 0.5
BUN level, mg/dL	16.5 ± 0.6	. . .	. . .	. . .	. . .	. . .
Ravn	. . .	15.8 ± 2.1	13.8 ± 1.9	10.8 ± 1.3	27.8 ± 15.2	33.3 ± 16.3
Angola	. . .	17.5 ± 0.6	15.5 ± 2.4	11.8 ± 0.5	15.0 ± 8.2	15.5 ± 6.5

Abbreviations: ALP, alkaline phosphatase; ALT, alanine transaminase; AST, aspartate transaminase; BUN, blood urea nitrogen; GGT, γ-glutamyl transpeptidase; TBIL, total bilirubin; WBC, white blood cells.

Spleen

On day 3, MARV antigen–positive mononuclear/dendritiform cells were observed for both MARV-Rav–infected GPs (3 of 4) and MARV-Ang–infected GPs (4 of 4; Figure 3*B* and 3*E*). Key differences on day 3 were immunoreactive cells scattered throughout the red pulp only for MARV-Rav–infected GPs and small clusters of immunoreactive cells within the red and white pulp for MARV-Ang–infected GPs. Corresponding congestion and tingible body macrophages were noted on H/E-stained sections of spleens from both MARV-Rav–infected GPs and MARV-Ang–infected GPs. Immunoreactive cells within the spleen peaked at day 3 for MARV-Ang–infected GPs (Figure 3*E*) and by day 5 for MARV-Rav–infected GPs (Figure 3*H*), with dispersion of MARV antigen–positive cells throughout the spleen by the end of the study. All animals, beginning on day 3 and continuing to death, had progressive lymphocyte depletion with tingible body macrophages, hemorrhage, and fibrin deposition within the white pulp. TUNEL staining of apoptotic populations within the splenic germinal centers increased over time, with peak intensity on day 5 for MARV-Ang–infected GPs (Figure 3*L*) and in terminal specimens for MARV-Rav–infected GPs (Figure 3*U*). Fibrin was scattered throughout the red pulp and clustered within the white pulp in MARV-Rav–infected GPs (Figure 4*B*). Fibrin immunolabeling of strands and aggregates within vessels, along the endothelium, and in clusters that disperse into the adjacent red and white pulp were present in MARV-Ang–infected GPs (Figure 4*C* and 4*D*).

Lymphoid Tissues

Beginning on day 5 and increasing in severity to the end of the study, lymphoid depletion was observed in mandibular (10 of 12 MARV-Rav–infected GPs and 11 of 12 MARV-Ang–infected GPs), axillary (8 of 12 and 8 of 12, respectively), and inguinal (8 of 12 and 8 of 12, respectively) lymph nodes. MARV antigen was noted in scattered mononuclear cells within the subcapsular and medullary sinuses of lymph nodes for both MARV-Rav and MARV-Ang groups. TUNEL staining of apoptotic populations within the mandibular lymph nodes increased over time, with peak intensity on day 5 for MARV-Ang–infected GPs and day 7 for MARV-Rav–infected GPs.

Adrenal Gland

MARV antigen–positive interstitial cells of the adrenal medulla were present in 4 of 4 MARV-Ang–infected GPs on day 3 and 4 of 4 MARV-Rav–infected GPs on day 5, yet no significant lesions were observed on H/E-stained sections. Subsequently, infection progressively extended into the interstitial cells of the cortex and cortical cells until death for both the MARV-Rav group (12 of 12 GPs) and the MARV-Ang group (12 of 12 GPs). Beginning on day 7, hemorrhage at the corticomedullary junction corresponded with immunoreactivity for both MARV-Rav–infected GPs (7 of 8) and MARV-Ang–infected GPs (7 of 8).

Lung

MARV antigen–positive alveolar macrophages and mononuclear cells within alveolar septae were observed on day 7 and at terminal time points for both MARV-Rav–infected GPs (7 of 8) and MARV-Ang–infected GPs (8 of 8), which corresponded with interstitial pneumonia (Supplementary Figure 2*B* and 2*C*).

Urogenital Tract

Beginning on day 7, MARV antigen was observed in submucosal interstitial cells and the transitional epithelium of the urinary bladder in MARV-Rav–infected GPs (3 of 8) and MARV-Ang–infected GPs (4 of 8; Supplemental Figure 1*E* and 1*F*). Lymphohistiocytic vasculitis of the urinary bladder submucosa was present in terminal specimens from MARV-Rav–infected animals, yet no lesions were noted in MARV-Ang–infected GPs. MARV antigen–positive mononuclear interstitial cells within the uterus, often surrounding small vessels and follicular thecal cells, were present at terminal time points of both MARV-Rav–infected GPs (2 of 2) and MARV-Ang–infected GPs (2 of 2), yet no significant lesions were observed on H/E-stained sections (data not shown).

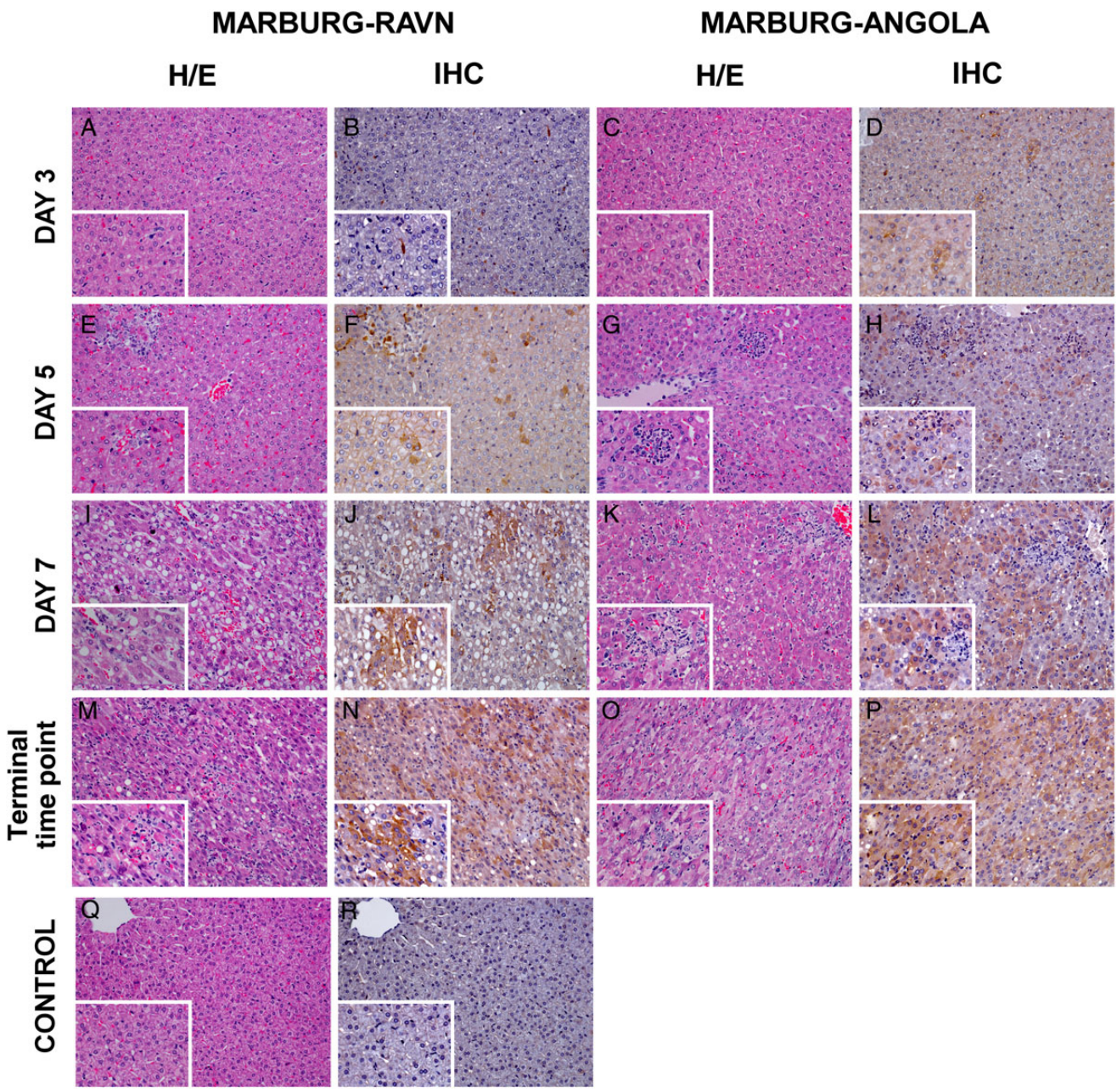

Figure 2. Histopathology of liver: Panels include Hemotoxylin & Eosin (H&E) MARV-Rav (*A, E, I,* and *M*) with corresponding anti-Marburg immunohistochemistry (IHC) (*B, F, J,* and *N*), H&E MARV Ang (*C, G, K,* and *O*) with corresponding anti-Marburg IHC (*D, H, L,* and *P*), and H&E control (*Q*) which has no significant lesions (NSL), nor any significant immunolabeling in corresponding anti-Marburg IHC (*R*). All images are 20x with 60x inserts. MARV-Rav-infected GP liver at day 3 (*A*) had NSL detected but had diffuse cytoplasmic immunolabeling of kupffer cells present (*B*). H&E of MARV-Rav-infected GP liver on day 5 (*E*) presented evidence of multifocal hepatocellular degeneration/necrosis and sinusoidal leukocytosis with diffuse cytoplasmic immunolabeling of Kupffer cells and small clusters of hepatocytes (*F*). Day 7 MARV-Rav-infected GP demonstrated progressive multifocal hepatocellular vacuolar degeneration/necrosis and sinusoidal leukocytosis on H&E (*I*) which was accompanied by diffuse cytoplasmic immunolabeling of Kupffer cells and clusters of hepatocytes (*J*). Terminal MARV-Rav-infected GP had advanced multifocal hepatocellular vacuolar degeneration/necrosis and sinusoidal leukocytosis (*M*) accompanied by diffuse cytoplasmic immunolabeling of Kupffer cells and sheets of hepatocytes (*N*). Day 3 MARV-Ang-infected GP had NSL on H&E (*C*) yet diffuse cytoplasmic immunolabeling of Kupffer cells and small clusters of hepatocytes was present (*D*). Day 5 MARV-Ang-infected GP had multifocal hepatocellular degeneration/necrosis and sinusoidal leukocytosis on H&E (*G*) which was associated with diffuse cytoplasmic immunolabeling of Kupffer cells and clusters of hepatocytes (*H*). Day 7 MARV-Ang-infected GP had marked multifocal hepatocellular vacuolar degeneration/necrosis and sinusoidal leukocytosis on H&E (*K*) with diffuse cytoplasmic immunolabeling of Kupffer cells and clusters of hepatocytes (*L*). Terminal MARV-Ang-infected GP had severe, multifocal hepatocellular vacuolar degeneration/necrosis and sinusoidal leukocytosis on H&E (*O*) associated with diffuse cytoplasmic immunolabeling of Kupffer cells and sheets of hepatocytes (*P*). Abbreviations: GP, guinea pig; MARV, Marburg virus.

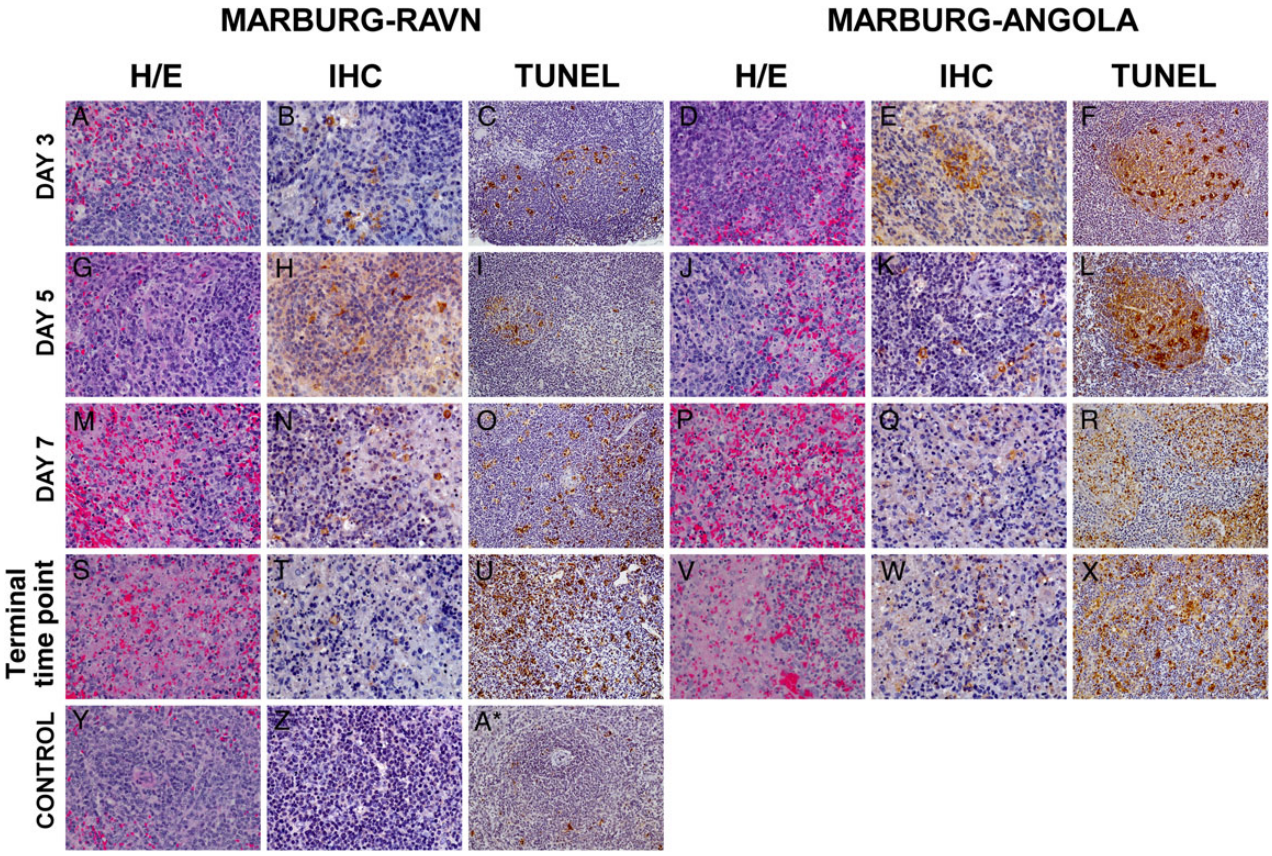

Figure 3. Histopathology of spleen: MARV Rav Hemotoxylin & Eosin (H&E) (*A*, *G*, *M*, and *S*), corresponding anti-Marburg immunohistochemistry (IHC) (*B*, *H*, *N*, and *T*), and TUNEL staining (*C*, *I*, *O*, and *U*). MARV-Ang H&E, (*D*, *J*, *P*, and *V*), corresponding anti-Marburg IHC (*E*, *K*, *Q*, and *W*), and TUNEL staining (*F*, *L*, *R*, and *X*). Control GP H&E (*Y*) had no significant lesions (NSL), corresponding anti-Marburg IHC had no significant immunolabeling (*Z*), and TUNEL staining presented minimal immunolabeling in the white pulp (A*). All H&E and IHC spleen images are 40×. TUNEL staining images are 20×. Day 3 MARV-Rav-infected GP had NSL on H&E (*A*), diffuse cytoplasmic immunolabeling of mononuclear cells in the red pulp (*B*) with minimal TUNEL staining in the white pulp (*C*). Day 5 MARV-Rav-infected GP demonstrated evidence of lymphoid depletion with tingible body macrophages within the white pulp on H&E (*G*), diffuse cytoplasmic anti-Marburg immunolabeling of clustered mononuclear cells in the red and white pulp (*H*), accompanied by minimal TUNEL staining in the white pulp (*I*). Day 7 MARV-Rav-infected GP displayed evidence of marked lymphoid depletion, fibrin deposition, and tingible body macrophages within the white pulp on H&E (*M*), diffuse cytoplasmic anti-Marburg immunolabeling of mononuclear cells in the red and white pulp (*N*), and moderate TUNEL staining in the white pulp (*O*). Terminal MARV-Rav-infected GP lymphoid depletion, fibrin deposition, hemorrhage and tingible body macrophages within the white pulp on H&E (*S*), diffuse cytoplasmic anti-Marburg immunolabeling of scattered mononuclear cells in the red and white pulp (*T*), and marked TUNEL staining in the white pulp (*U*). Day 3 MARV-Ang-infected GP had NSL on H&E (*D*), diffuse cytoplasmic anti-Marburg immunolabeling of clustered mononuclear cells in the red and white pulp (*E*), and moderate TUNEL staining in the white pulp (*F*). Day 5 MARV-Ang-infected GP had evidence of lymphoid depletion with tingible body macrophages within the white pulp (*J*), diffuse cytoplasmic anti-Marburg immunolabeling of mononuclear cells in the red and white pulp (*K*), and moderate TUNEL staining in the white pulp (*L*). Day 7 MARV-Ang-infected GP lymphoid depletion, fibrin deposition, and tingible body macrophages within the white pulp on H&E (*P*), diffuse cytoplasmic anti-Marburg immunolabeling of mononuclear cells in the red and white pulp (*Q*), marked TUNEL staining in the white pulp (*R*). MARV-Ang-infected GP spleen, terminal (*V*) lymphoid depletion, fibrin deposition, hemorrhage, and tingible body macrophages within the white pulp, diffuse cytoplasmic anti-Marburg immunolabeling of scattered mononuclear cells in the red and white pulp (*W*), and marked immunolabeling in the white pulp (*X*). Abbreviations: GP, guinea pig; MARV, Marburg virus.

Gastrointestinal Tract

A focal gastric ulceration was noted in a terminal specimen from 1 MARV-Ang GP. Beginning on day 7, with progression to death, lymphoid depletion in MARV-Rav GPs was noted in the thymus (7 of 8 animals), ileocecal junction (8 of 8), and duodenum (8 of 8); similar findings were also observed in MARV-Ang–infected GPs (8 of 8, 8 of 8, and 6 of 8, respectively). TUNEL staining of apoptotic populations within the lamina propria of the duodenum at death of a MARV-Ang–infected GP was most striking, extending from the villar tips to the submucosa, compared with that of a MARV-Rav–infected GP, which extended approximately one fourth of the way down the villar tip (Supplementary Figure 2*G*–*I*).

Coagulation Parameters

Prothrombin times began to extend significantly beginning at day 3 and continued to lengthen throughout the course of disease. Activated partial thromboplastin times (APTTs) were not

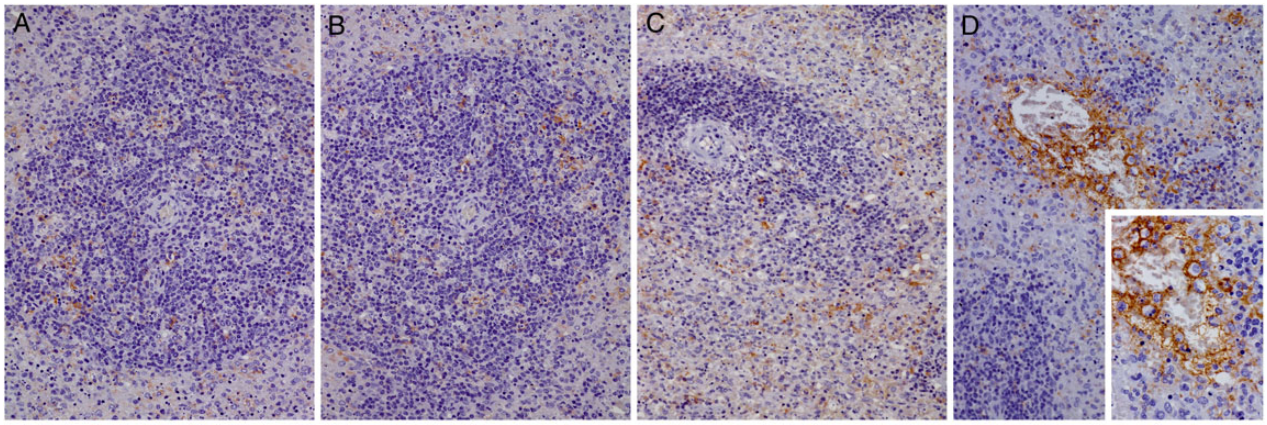

E

SCALE: LOW HIGH

	PARAMETER	CONTROL		DAY 1		DAY 3		DAY 5		DAY 7		Terminal Time Point		VIRUS
		MEAN	SD	MEAN	SD	MEAN	SD	MEAN	SD	MEAN	SD	MEAN	SD	
COAGULATION PARAMETERS	PT, s	3.8E+01	4.8E-01	3.0E+01	1.2E+01	4.3E+01	7.5E+00	6.3E+01	6.4E+00	>70		>70		RAVN
				3.7E+01	5.6E-01	4.2E+01	3.4E+00	5.5E+01	7.8E+00	>70		>70		ANGOLA
	APTT, s	2.8E+01	4.9E+00	2.2E+01	2.6E+00	2.4E+01	3.3E+00	2.7E+01	4.5E+00	4.8E+01	1.1E+01	9.1E+01	2.3E+01	RAVN
				1.8E+01	2.1E+00	2.8E+01	7.6E+00	2.7E+01	4.9E+00	5.7E+01	1.2E+01	6.4E+01	8.1E+00	ANGOLA
	TT, s	3.6E+01	1.8E+00	2.5E+01	2.5E+00	2.2E+01	5.6E+00	1.6E+01	8.6E-01	1.5E+01	1.5E+00	2.0E+01	4.4E+00	RAVN
				3.1E+01	1.8E+00	2.5E+01	4.5E+00	1.8E+01	3.7E+00	1.7E+01	3.2E+00	2.1E+01	4.0E+00	ANGOLA
	Fibrinogen, mg/dL	1.8E+02	2.2E+01	2.5E+02	2.2E+01	2.9E+02	6.5E+01	3.6E+02	1.7E+01	3.9E+02	3.3E+01	3.0E+02	4.8E+01	RAVN
				2.1E+02	1.0E+01	2.5E+02	3.3E+01	3.4E+02	6.8E+01	3.6E+02	6.9E+01	2.9E+02	4.7E+01	ANGOLA
	Protein C, % activity	9.7E+01	6.1E+00	9.6E+01	8.0E+00	8.1E+01	1.2E+01	8.1E+01	9.1E+00	7.3E+01	3.8E+00	6.5E+01	1.6E+01	RAVN
				9.4E+01	1.3E+01	9.8E+01	8.0E+00	8.9E+01	1.1E+01	8.3E+01	1.1E+01	6.2E+01	5.0E+00	ANGOLA
	Thrombin-thrombomodulin complexes, pg/mL	3.5E+02	7.1E+02	2.0E+03	2.6E+03	3.1E+03	5.3E+03	7.3E+03	6.1E+03	8.0E+03	2.5E+03	3.6E+03	1.7E+03	RAVN
				9.9E+02	1.2E+03	4.2E+02	8.5E+02	5.6E+03	2.1E+03	6.0E+03	1.0E+03	5.4E+03	5.3E+03	ANGOLA
	Bradykinin, pg/mL	1.1E+01	2.1E+01	2.1E+01	1.6E+01	2.7E+01	1.9E+01	5.4E+01	2.6E+01	6.3E+01	2.9E+01	7.5E+01	7.4E+00	RAVN
				2.8E+01	2.2E+01	3.4E+01	1.2E+01	4.7E+01	4.0E+01	6.4E+01	7.5E+00	4.6E+01	1.1E+01	ANGOLA
	Prekalikrein, pg/mL	1.9E+01	1.4E+01	9.8E+00	1.1E+01	0.0E+00	0.0E+00	5.0E+00	6.4E+00	1.3E+01	1.5E+01	2.0E+01	1.7E+01	RAVN
				0.0E+00	0.0E+00	5.6E+00	1.1E+01	1.0E+01	1.2E+01	3.8E+01	4.6E+00	2.6E+01	9.3E+00	ANGOLA
	PAI-1, ng/mL	2.2E+01	1.5E+01	1.7E+01	2.0E+01	1.5E+01	2.9E+01	6.3E+01	2.1E+01	1.2E+02	2.6E+01	1.3E+02	2.0E+01	RAVN
				2.0E+01	1.5E+01	2.9E+01	2.6E+01	3.2E+01	1.4E+01	1.4E+02	2.9E+01	9.9E+01	2.7E+01	ANGOLA
	TAFI, ng/mL	0.0E+00	0.0E+00	0.0E+00	0.0E+00	2.5E+01	1.8E+01	5.0E+01	3.4E+01	2.3E+01	1.3E+01	6.2E+01	4.3E+01	RAVN
				0.0E+00	0.0E+00	2.9E+00	5.7E+00	3.5E+00	7.1E+00	5.9E+01	4.4E+01	5.8E+01	3.0E+01	ANGOLA
	Tissue factor, pg/mL	5.9E+01	2.9E+00	4.9E+01	2.9E+00	5.4E+01	1.7E+00	4.9E+01	6.7E+00	3.9E+01	4.3E+00	2.5E+01	2.0E+01	RAVN
				5.3E+01	2.2E+00	5.2E+01	4.5E+00	4.7E+01	1.1E+01	3.9E+01	1.7E+01	2.0E+01	3.8E+00	ANGOLA
	VWF, ng/mL	1.5E+02	2.3E+01	1.3E+02	3.9E+01	1.2E+02	3.0E+01	1.4E+02	6.2E+01	1.8E+02	8.7E+01	2.6E+02	5.4E+01	RAVN
				1.4E+02	3.4E+01	1.4E+02	1.0E+01	7.3E+01	1.8E+01	2.9E+02	5.8E+01	2.3E+02	5.6E+01	ANGOLA
INFLAMMATORY MARKERS	Prostaglandin E2, pg/mL	2.1E+01	1.3E+01	1.8E+01	1.4E+01	1.5E+01	7.6E+00	4.7E+01	1.1E+01	8.8E+01	2.0E+01	6.4E+01	5.0E+00	RAVN
				1.3E+01	8.7E+00	6.8E+00	3.3E+00	2.1E+01	1.2E+01	6.5E+01	6.4E+00	6.7E+01	4.8E+00	ANGOLA
	Leukotriene B4, pg/mL	1.8E+02	9.0E+01	1.9E+02	2.0E+01	3.9E+02	9.9E+01	1.4E+02	41..40	3.3E+02	1.0E+02	5.2E+02	1.9E+02	RAVN
				3.7E+02	1.2E+02	2.6E+02	4.8E+01	4.7E+02	2.4E+02	5.1E+02	2.9E+02	8.7E+02	3.3E+02	ANGOLA
	Cysteinal leukotrienes, pg/mL	3.8E+01	1.8E+01	5.1E+01	1.1E+00	8.2E+01	3.2E+01	4.9E+01	2.8E+01	2.1E+02	5.2E+01	3.6E+02	4.2E+01	RAVN
				6.3E+01	1.5E+01	4.2E+01	2.2E+01	1.0E+02	7.2E+01	1.7E+02	5.4E+01	3.4E+02	7.2E+01	ANGOLA
	Thromboxane B2, pg/mL	3.4E+02	1.1E+02	3.5E+02	1.1E+02	7.4E+02	1.2E+02	7.8E+02	1.5E+02	6.7E+02	1.4E+02	1.2E+03	1.8E+02	RAVN
				4.0E+02	7.1E+01	4.9E+02	1.1E+02	5.4E+02	8.8E+01	4.6E+02	5.9E+01	4.5E+02	7.1E+01	ANGOLA
	6-keto prostaglandin F1α, pg/mL	9.3E+00	3.3E+00	9.1E+00	1.4E+00	3.7E+01	1.4E+01	4.1E+01	1.5E+01	9.9E+01	4.0E+01	3.0E+02	1.9E+02	RAVN
				1.3E+01	3.5E+00	1.4E+01	3.3E+00	9.2E+01	8.3E+01	9.4E+01	6.5E+01	2.9E+02	2.9E+02	ANGOLA
	TGF-β, pg/mL	2.1E+00	4.2E+00	2.0E+00	4.0E+00	1.2E+00	1.3E+00	6.8E+00	7.4E+00	1.3E+01	8.0E+00	1.8E+01	5.2E+00	RAVN
				0.0E+00	0.0E+00	0.0E+00	0.0E+00	1.2E+00	1.8E+00	1.7E+01	5.1E+00	1.9E+01	6.6E+00	ANGOLA
	HMGB-1, pg/mL	2.0E+02	1.4E+02	2.3E+03	1.6E+03	3.0E+03	6.2E+02	2.5E+03	7.1E+02	1.5E+03	4.5E+02	1.1E+03	1.4E+03	RAVN
				1.1E+03	4.5E+02	4.7E+02	3.1E+02	1.9E+03	5.6E+02	3.3E+02	6.5E+02	4.2E+02	4.3E+02	ANGOLA
	TNF-α, pg/mL	1.1E+02	4.6E+01	2.1E+01	2.8E+01	0.0E+00	0.0E+00	2.2E+02	2.6E+02	1.7E+02	4.2E+01	4.1E+02	1.0E+02	RAVN
				3.8E+01	3.8E+01	5.6E+01	6.6E+01	1.0E+02	9.2E+01	3.8E+02	8.3E+01	4.7E+02	9.5E+01	ANGOLA
	IL-6, pg/mL	1.4E+01	2.8E+01	6.3E+01	9.1E+01	2.7E+01	5.3E+01	1.4E+02	9.7E+01	4.1E+02	1.1E+02	3.2E+02	1.7E+02	RAVN
				0.0E+00	0.0E+00	5.9E+00	1.2E+01	2.1E+02	5.2E+01	3.7E+02	2.4E+02	5.8E+02	1.8E+02	ANGOLA
	NO, μM nitrite	2.1E-01	4.3E-01	0.0E+00	0.0E+00	0.0E+00	0.0E+00	1.5E+01	1.2E+01	3.0E+01	1.8E+01	6.9E+01	6.9E+01	RAVN
				0.0E+00	0.0E+00	0.0E+00	0.0E+00	8.1E+00	1.4E+01	9.4E+01	4.5E+01	1.3E+02	8.6E+01	ANGOLA

Figure 4. Fibrin specific immunohistochemistry of GP spleens: Control GP had no significant immunolabeling (*A*). Day 7 MARV-Rav-infected GP had minimal anti-fibrin immunolabeling scattered throughout the red pulp and clustered in the white pulp (*B*). Day 7 MARV-Ang-infected GP with anti-fibrin immunolabeling scattered throughout the red pulp and clustered in the white pulp (*C*). Inset depicts representative immunolabeling of fibrin strands and aggregates surrounding red and white blood cells within the vessel, along the endothelium, and clusters that disperse into the adjacent red and white pulp (*D*). All 20× with 60× insert in (*D*). Heat map and expression levels of coagulation factors and inflammatory molecules detected through the course of infection (*E*). Abbreviations: APTT, activated partial thromboplastin times; GP, guinea pig; HMGB-1, high-mobility group B1; IL-6, interleukin 6; MARV, Marburg virus; NO, nitric oxide; PAI-1, plasminogen activator inhibitor 1; PT, partial thrombin; SD, standard deviation; TAFI, thrombin-activated fibrinolysis inhibitor; TGF, transforming growth factor; TNF, tumor necrosis factor; TT, thrombin time; VWF, Von Willebrand factor.

extended until late in disease, beginning on day 7. Beginning on day 1, decreases in thrombin times corresponded with increases in fibrinogen content throughout the disease course. Circulating protein C activity and tissue factor levels progressively decreased;

however, plasminogen activator inhibitor 1 (PAI-1) and von Willebrand factor levels were markedly increased in late disease. The mean thrombin-activated fibrinolysis inhibitor (TAFI) level began to increase markedly on day 3 in MARV-Rav–infected GPs and stayed elevated through death. Conversely, MARV-Ang–infected GPs did not have an increased mean level of TAFI until late in disease. Interestingly, circulating tissue factor levels decreased gradually until the time of death. Bradykinin levels gradually increased to approximately 6-fold higher than those in control animals at late points in disease. Conversely, prekallikrein levels were severely depressed until late in the disease course, when, at day 7, a striking increase was recorded in MARV-Ang–infected GPs but not in MARV-Rav–infected animals. Circulating levels of thrombin in complex with thrombomodulin were noted beginning on day 1 and increased throughout the disease course for both strains (Figure 4*E*).

Circulating Eicanosoid, Cytokine, and Nitric Oxide Production

Mean levels of prostaglandin E2 began to decrease on day 1, with a continued decrease to day 3. Beginning on day 5, however, marked increases were noted in mean values, with the terminal mean value approximately 3 times that of control animals. The mean leukotriene B4 value was elevated in MARV-Ang animals on day 1 and tended to increase over the disease course to approximately 4 times the level in control animals. MARV-Rav–infected animals demonstrated a similar trend, beginning on day 3, but with comparatively muted mean levels. Mean cysteinal leukotriene levels gradually increased throughout the course of infection, beginning on day 5. Thromboxane B2 levels were elevated in MARV-Rav–infected animals beginning on day 3 and continuing through terminal time points; conversely, MARV-Ang–infected animals did not have significant difference in levels of this eicansoid. Prostacyclin levels were measured via the stable metabolite 6-keto-prostaglandin F1a and were first elevated in MARV-Rav–infected animals beginning on day 3; MARV-Ang–infected animals demonstrated a marked increase on day 5. Transforming growth factor β, interleukin 6, and tumor necrosis factor α values were marked late in disease through death. Very soon after infection, mean levels of HMGB-1 were higher in MARV-Rav–infected GPs, compared with MARV-Ang–infected GPs, yet both were markedly elevated as compared to those in control animals throughout the study. Circulating nitrite levels were increased in both species, beginning on day 5; however, striking increases were recorded in MARV-Ang–infected animals in late disease (Figure 4*E*).

DISCUSSION

The increased frequency and severity of filovirus outbreaks in recent years underscores the dire need for medical countermeasures. The development of rodent models that faithfully represent MHF processes yet maintain predictive power for filovirus-specific countermeasures could facilitate scale up of screening efforts of these medical interventions and thereby restrict precious primate resources to only the most likely candidate countermeasures. Inbred rodent models are commonly used to model a variety of disease processes but have limitations in regard to their well-documented depressed immune capacity. This caveat is a major shortcoming for vaccines and therapeutic development, which maintain heavy reliance on various aspects of host immunity for efficacy. To further complicate the issue, limited descriptions of coagulopathies or vascular leak in rodent models of MHF exist, thereby limiting the power of these models.

To address the need for improved rodent models, we presented 2 outbred GP models that demonstrate not only hallmark features of MHF, but also provide systematic evidence for differences in pathogenicity among phylogenetically diverse MARV strains. Both models recapitulate important aspects of NHP and human MHF pathogenic features, including fever, weight loss, and early infection of macrophage/dendritiform cells, followed by remarkable splenic and hepatic pathology, lymphocyte apoptosis, neutrophilia, thrombocytopenia, and marked granulocytosis. Perturbations in serum biochemistry findings in NHP and human MHF were also similar, specifically in regard to marked increases in liver-associated enzyme levels, proinflammatory cytokine levels, nitric oxide species and hypoalbuminemia. This work also details a severe coagulopathy, which includes increased prothrombin and APTTs, decreased thrombin times, decreased protein C activity, marked fibrinogen deregulation, increased prostacyclin, thromboxane, von Willebrand factor, PAI-1, and circulating thrombin-thrombomodulin complex levels, and deposition of fibrin in tissues, all of which have been demonstrated in MHF in NHPs and humans [15–19]. Although decreased serum tissue factor was also documented, we have yet to clarify whether levels are elevated in tissues, as previously documented in NHPs [20].

Given the similarities in pathogenesis between viral hemorrhagic fever and sepsis [21, 22], we probed this model for several pathologically relevant phenomena that are important in bacterial sepsis. We detected evidence for activation of the kallikrein-kinin system and disruption of fibrinolysis processes, as evidenced by abrogated bradykinin, prekallikrein, and TAFI metabolism. Deregulation of circulating eicanosoids has also been associated with sepsis [23, 24]. Accordingly, we documented deregulation of several important species of prostaglandins and leukotrienes late in disease. Recent work in sepsis has also suggested the importance of proinflammatory cytokine/transcription factor HMGB-1 in disease severity [25, 26]. Our data suggest a role for this molecule in early MHF that may lend to differences in pathogenesis between MARV strains.

Prior work with the Musoke strain of MARV identified several mutations necessary for lethality in strain 13 GPs; however, sequencing of the GPA MARVs from this work revealed multiple changes, of which none had been previously described [27].

Both MARV strains adopted genetic mutations that resulted in amino acid changes within the VP40 proteins; however, only MARV-Ang had changes in VP24, a protein recognized to be important in formation of infectious particles and interaction with cytoprotective antioxidant response pathways [28, 29]. Given the higher viral burden in tissues and plasma, marked increases in severe inflammation, and shorter mean time to death, this finding suggests that VP24 is a potential molecular landmark responsible for virulence differences between MARV species. The recently developed reverse genetics system for MARV will allow for a more mechanistic approach to identify which mutations directly contribute to pathogenesis in these models [30, 31]. This study represents the first systematic pathogenesis study of MARV strains in vivo and demonstrates the need for strain consideration when developing countermeasures against MARV.

Supplementary Data

Supplementary materials are available at *The Journal of Infectious Diseases* online (http://jid.oxfordjournals.org). Supplementary materials consist of data provided by the author that are published to benefit the reader. The posted materials are not copyedited. The contents of all supplementary data are the sole responsibility of the authors. Questions or messages regarding errors should be addressed to the author.

Notes

Acknowledgments. We thank Kerry Graves, Natalie Dobias, and the University of Texas Medical Branch (UTMB) histology core, for assistance with tissue preparations; and Jessica Graber, Daniel Deer, Krystle Agans, and the UTMB sequencing core, for technical and administrative support during these studies.

Disclaimer. The opinions, interpretations, conclusions, and recommendations contained herein are those of the authors and are not necessarily endorsed by the University of Texas Medical Branch at Galveston or the National Institute of Allergy and Infectious Diseases (NIAID), National Institutes of Health (NIH).

Financial support. This work was supported by the Department of Microbiology and Immunology, University of Texas Medical Branch at Galveston (to T. W. G.); and the Intramural Research Program of the NIAID, NIH (to H. E.).

Potential conflicts of interest. All authors: No reported conflicts.

All authors have submitted the ICMJE Form for Disclosure of Potential Conflicts of Interest. Conflicts that the editors consider relevant to the content of the manuscript have been disclosed.

References

1. Colebunders R, Tshomba A, Van Kerkhove MD, et al. Marburg hemorrhagic fever in Durba and Watsa, Democratic Republic of the Congo: clinical documentation, features of illness, and treatment. J Infect Dis **2007**; 196(suppl 2):S148–53.
2. Towner JS, Khristova ML, Sealy TK, et al. Marburgvirus genomics and association with a large hemorrhagic fever outbreak in Angola. J Virol **2006**; 80:6497–516.
3. Johnson ED, Johnson BK, Silverstein D, et al. Characterization of a new Marburg virus isolated from a 1987 fatal case in Kenya. Arch Virol Suppl **1996**; 11:101–14.
4. Smith DH, Johnson BK, Isaacson M, et al. Marburg-virus disease in Kenya. Lancet **1982**; 1:816–20.
5. Ursic-Bedoya R, Mire CE, Robbins M, et al. Protection against lethal Marburg virus infection mediated by lipid encapsulated small interfering RNA. J Infect Dis **2014**; 209:562–70.
6. Daddario-DiCaprio KM, Geisbert TW, Geisbert JB, et al. Cross-protection against Marburg virus strains by using a live, attenuated recombinant vaccine. J Virol **2006**; 80:9659–66.
7. Alves DA, Glynn AR, Steele KE, et al. Aerosol exposure to the angola strain of marburg virus causes lethal viral hemorrhagic Fever in cynomolgus macaques. Vet Pathol **2010**; 47:831–51.
8. Geisbert TW, Daddario-DiCaprio KM, Geisbert JB, et al. Marburg virus Angola infection of rhesus macaques: pathogenesis and treatment with recombinant nematode anticoagulant protein c2. J Infect Dis **2007**; 196(suppl 2):S372–81.
9. Warfield KL, Bradfute SB, Wells J, et al. Development and characterization of a mouse model for Marburg hemorrhagic fever. J Virol **2009**; 83:6404–15.
10. Warfield KL, Swenson DL, Negley DL, Schmaljohn AL, Aman MJ, Bavari S. Marburg virus-like particles protect guinea pigs from lethal Marburg virus infection. Vaccine **2004**; 22:3495–502.
11. Swenson DL, Warfield KL, Larsen T, Alves DA, Coberley SS, Bavari S. Monovalent virus-like particle vaccine protects guinea pigs and nonhuman primates against infection with multiple Marburg viruses. Expert Rev Vaccines **2008**; 7:417–29.
12. Wahl-Jensen V, Bollinger L, Safronetz D, de Kok-Mercado F, Scott DP, Ebihara H. Use of the Syrian hamster as a new model of ebola virus disease and other viral hemorrhagic fevers. Viruses **2012**; 4:3754–84.
13. Thi EP, Mire CE, Ursic-Bedoya R, et al. Marburg virus infection in nonhuman primates: Therapeutic treatment by lipid-encapsulated siRNA. Sci Transl Med **2014**; 6:250ra116.
14. Ursic-Bedoya R, Mire CE, Robbins M, et al. Protection Against Lethal Marburg Virus Infection Mediated by Lipid Encapsulated Small Interfering RNA. J Infect Dis **2014**; 209:562–70.
15. McElroy AK, Erickson BR, Flietstra TD, et al. Biomarker correlates of survival in pediatric patients with Ebola virus disease. Emerg Infect Dis **2014**; 20:1683–90.
16. McElroy AK, Erickson BR, Flietstra TD, et al. Von Willebrand Factor Is Elevated in Individuals Infected with Sudan Virus and Is Associated with Adverse Clinical Outcomes. Viral Immunol **2015**; 28:71–3.
17. Fisher-Hoch SP, Platt GS, Neild GH, et al. Pathophysiology of shock and hemorrhage in a fulminating viral infection (Ebola). J Infect Dis **1985**; 152:887–94.
18. Geisbert TW, Young HA, Jahrling PB, et al. Pathogenesis of Ebola hemorrhagic fever in primate models: evidence that hemorrhage is not a direct effect of virus-induced cytolysis of endothelial cells. Am J Pathol **2003**; 163:2371–82.
19. Geisbert TW, Hensley LE, Gibb TR, Steele KE, Jaax NK, Jahrling PB. Apoptosis induced in vitro and in vivo during infection by Ebola and Marburg viruses. Lab Invest **2000**; 80:171–86.
20. Geisbert TW, Hensley LE, Larsen T, et al. Pathogenesis of Ebola hemorrhagic fever in cynomolgus macaques: evidence that dendritic cells are early and sustained targets of infection. Am J Pathol **2003**; 163:2347–70.
21. Bray M, Mahanty S. Ebola hemorrhagic fever and septic shock. J Infect Dis **2003**; 188:1613–7.
22. Steinberg BE, Goldenberg NM, Lee WL. Do viral infections mimic bacterial sepsis? The role of microvascular permeability: A review of mechanisms and methods. Antiviral Res **2012**; 93:2–15.
23. Bruegel M, Ludwig U, Kleinhempel A, et al. Sepsis-associated changes of the arachidonic acid metabolism and their diagnostic potential in septic patients. Crit Care Med **2012**; 40:1478–86.
24. Feuerstein G, Hallenbeck JM. Prostaglandins, leukotrienes, and platelet-activating factor in shock. Annu Rev Pharmacol Toxicol **1987**; 27: 301–13.
25. Sunden-Cullberg J, Norrby-Teglund A, Rouhiainen A, et al. Persistent elevation of high mobility group box-1 protein (HMGB1) in patients with severe sepsis and septic shock. Crit Care Med **2005**; 33:564–73.
26. Bae JS. Role of high mobility group box 1 in inflammatory disease: focus on sepsis. Arch Pharm Res **2012**; 35:1511–23.

27. Lofts LL, Ibrahim MS, Negley DL, Hevey MC, Schmaljohn AL. Genomic differences between guinea pig lethal and nonlethal Marburg virus variants. J Infect Dis **2007**; 196(suppl 2):S305–12.
28. Bamberg S, Kolesnikova L, Moller P, Klenk HD, Becker S. VP24 of Marburg virus influences formation of infectious particles. J Virol **2005**; 79:13421–33.
29. Edwards MR, Johnson B, Mire CE, et al. The Marburg virus VP24 protein interacts with Keap1 to activate the cytoprotective antioxidant response pathway. Cell Rep **2014**; 6:1017–25.
30. Albarino CG, Uebelhoer LS, Vincent JP, et al. Development of a reverse genetics system to generate recombinant Marburg virus derived from a bat isolate. Virology **2013**; 446:230–7.
31. Albarino CG, Wiggleton Guerrero L, Spengler JR, et al. Recombinant Marburg viruses containing mutations in the IID region of VP35 prevent inhibition of Host immune responses. Virology **2014**; 476C:85–91.
32. Fiddler RN. Collaborative study of modified AOAC method of analysis for nitrite in meat and meat products. J Assoc Off Anal Chem **1977**; 60:594–9.